

Genetic Polymorphisms in Human Proton-Dependent Dipeptide Transporter
PEPT1: Implications for the Functional Role of Pro⁵⁸⁶

Eric Y. Zhang^{*}, Dong-Jing Fu[‡], Youngeen A. Pak^{*}, Trent Stewart[‡], Nitai
Mukhopadhyay[§], Steven A. Wrighton and Kathleen M. Hillgren^{*†}

From ^{*}Discovery Drug Disposition & New Technology, [‡] Functional Genomics, [§]
Diagnostics & Experimental Medicine, Lilly Research Laboratories, Eli Lilly and
Company. Indianapolis, IN 46285.

Running title: Polymorphisms of human PEPT1

† Corresponding author

Kathleen M. Hillgren, Ph. D.

Lilly Research Laboratories, Lilly Corporate Center, Indianapolis, IN 46285

Tel: +1-317-433-6678

Fax: +1-317-433-5432

Email: Kathleen_M_Hillgren@lilly.com

Keywords: peptide transporter, PEPT1, polymorphism, peptidomimetics

Abbreviations: PEPT1, the small intestine proton-dependent dipeptide transporter; cSNP, coding region single nucleotide polymorphism; RT-PCR, reverse transcription-polymerase chain reaction; bp, base pair; TM, transmembrane segment; PBS, phosphate-buffered saline.

The number of text pages: 24

The number of tables: 4

The number of figures: 6

The number of references: 40

The number of words in the *Abstract*: 196

The number of words in the *Introduction*: 588

The number of words in the *Discussion*: 1938

A recommended section assignment:

Absorption, Distribution, Metabolism, & Excretion

Abstract

The human proton-dependent dipeptide transporter (PEPT1, gene SLC15A1) is important for intestinal absorption of di- and tri-peptides and a variety of peptidomimetic compounds. Utilizing a DNA polymorphism discovery panel of 44 ethnically diverse individuals, nine non-synonymous and four synonymous coding-region single-nucleotide polymorphisms (cSNPs) were identified in PEPT1. HeLa cells were transiently transfected with plasmids constructed by site-directed mutagenesis for each of the 9 non-synonymous variants. Quantitative PCR showed that the mRNA transcription level of all of the mutants were comparable to the mRNA transcription level of the reference sequence in transfected HeLa cells. Functional analysis in transiently transfected HeLa cells revealed that all non-synonymous variants retained similar pH-dependent activity and K_t values for Gly-Sar uptake as the reference PEPT1. In addition, a group of seven peptide-like drugs showed inhibitory effect on Gly-Sar uptake by these variants comparable to the reference, suggesting conserved drug recognition. Of the 9 non-synonymous SNPs, a single SNP (P586L) demonstrated significantly reduced transport capacity as evidenced by a much lower V_{max} value. This was consistent with lower immunoactive protein level (Western analysis) and lower plasma membrane expression (immunocytochemical analysis). Therefore, Pro⁵⁸⁶ may have profound effect on PEPT1 translation, degradation and/or membrane insertion.

Introduction

In recent years, molecular characterization of numerous drug transporters has greatly expanded our understanding of cellular mechanisms of drug disposition. By controlling the cellular entry and exit of compounds, drug transporters have been recognized as important determinants of drug absorption, distribution and elimination. In the small intestine, nutrient transporters, such as the intestinal peptide transporter, are involved in the active absorptive influx of xenobiotics (i.e. β -lactam antibiotics) from the intestinal lumen to the portal blood (Dantzig, 1997). In opposition to compound influx, P-glycoprotein is responsible for the active efflux of drugs (i.e. digoxin) from intestinal epithelial cells back to the lumen (Sababi et al., 2001). In the liver, there is a large set of influx and efflux transporters that play important roles in the clearance and excretion of drugs. For example, pravastatin (Tokui et al., 1999) is extracted efficiently from portal vein by the liver through the organic anion transporting polypeptide C (OATP-C). In the kidney, antiviral reagents such as adefovir and cidofovir can undergo active secretion by the organic anion transporter (Ho et al., 2000).

Genetic variations in the enzymes responsible for phase I and II metabolism have been shown to be a source of interindividual variability in drug effect and disposition (Meyer and Zanger, 1997; Hayes and Strange, 2000; Mackenzie et al., 2000; Rodrigues and Rushmore, 2002). Therefore, it is not surprising that genetic variations in drug transporter genes have been also implicated in changes of transporter expression level and function, which could affect drug disposition (Hoffmeyer et al., 2000; Ito et al., 2001; Tirona et al., 2001;

Leabman et al., 2002). For example, alterations in the disposition of fexofenadine (Kim et al., 2001) and digoxin (Hoffmeyer et al., 2000) were found linked to polymorphisms in P-glycoprotein. Most recently, it has been shown that one commonly occurring SNP (T521C) in the organic anion transporting polypeptide C (OATP-C) is likely to be related to altered pharmacokinetics of pravastatin in a Japanese population (Nishizato et al., 2003).

The intestinal proton- dependent dipeptide transporter, PEPT1, was first cloned from rabbit (Fei et al., 1994) and subsequently from human, mouse and rat (Liang et al., 1995; Saito et al., 1995; Fei et al., 2000). The nucleotide and primary amino acid sequence of PEPT1 is highly homologous across species and has a high transport capacity in small intestine. In addition to its naturally occurring substrates, di- and tri-peptides, PEPT1 is capable of actively transporting a variety of chemically diverse compounds, including β -lactam antibiotics, renin inhibitors and angiotensin converting enzyme (ACE) inhibitors (Rubio-Aliaga and Daniel, 2002). Because of the broad substrate specificity of PEPT1, a prodrug approach, by which a poorly bioavailable drug is modified to be transported by PEPT1, has been intensively investigated as a promising strategy to improve oral absorption of certain molecules (Balimane et al., 1998; Steffansen et al., 1999; Friedrichsen et al., 2001; Thomsen et al., 2003). It is anticipated that with the unfolding of substrate structural requirements of PEPT1, more rationally designed peptidomimetic molecules and prodrugs targeting to PEPT1 will be generated in the future.

Despite increasing efforts in investigating PEPT1 as a possible drug delivery system for small peptides and peptide-like compounds, little information is available regarding potential functional consequence of genetic variations of human PEPT1. In the present study, we identified 13 cSNPs in PEPT1 utilizing a DNA polymorphism discovery panel and studied their function *in vitro*. We show that all PEPT1 non-synonymous variants identified in this study have conserved substrate recognition. In addition, one variant (P586L) was associated with profound reduction in uptake capacity.

Methods

Materials

[Glycyl-1,2-¹⁴C]-glycylsarcosine (Gly-Sar) (110 mCi/mmol) was purchased from Moravek Biochemicals, Inc (Brea, CA). BCA protein assay kit was purchased from Pierce (Rockford, IL). Rabbit anti-human PepT1 polyclonal antiserum was custom-made by Zymed Laboratories (South San Francisco, CA) and prepared from animals injected with a peptide corresponding to the last 17 amino acid residues of human PEPT1 (CKSNPYFMGANSQKQM). Rabbit anti-calnexin polyclonal antibody was from Stressgen (Victoria, BC Canada). Unlabeled Gly-Sar, glycine, cefadroxil, captopril, cephalixin, enalapril, L-3, 4-dihydroxyphenyl alanine (L-DOPA), bestatin, and 5-aminolevulinic acid hydrochloride (ALA) were from Sigma (St. Louis, MO). HeLa cells (CCL-2) were obtained from the American Type Culture Collection (Manassas, VA). Cells were grown in Dulbecco's modified Eagle's medium containing 10% fetal calf serum, 4.5 g/L glucose, 110 mg/L sodium pyruvate, 584 mg/L L-glutamine, 0.1 mM non-essential amino acids, 100 units/ml penicillin, and 100 µg/ml streptomycin (Invitrogen, Carlsbad, CA) at 37°C in a humidified atmosphere with 5% CO₂.

SNP identification

PEPT1 mRNA sequence was obtained from GeneBank (Accession No. NM_005073). This sequence was designated as the reference PEPT1 in the study. Determination of coding sequence, untranslated regions and intronic regions was based on annotation in the GeneBank databases. Samples used for polymorphism discovery were obtained from a DNA polymorphism discovery

panel (M44PDR) from Coriell Cell Repositories (Camden, NJ). The panel consists of genomic DNA isolated from 44 unrelated individuals of different ethnicity, including 11 European-American, 11 African-American, 11 Asian-American, 6 Mexican-American, and 5 native Americans.

PCR assays were designed to obtain a product of ~ 500 bp that includes 50-80 bp of flanking intronic sequence. The genomic PCR reaction was carried out with DNA polymerase AmpliTaq Gold (Applied Biosystems, Foster City, CA). A 25 μ l PCR reaction was performed containing 100 ng genomic DNA, 1 unit AmpliTaq Gold, 2.5 pmol forward primer, 2.5 pmol reverse primer, 0.2 mM dNTPs, 1 \times AmpliTaq Gold buffer, and 4% DMSO. The reaction mixture was denatured at 94°C for 3 min, followed by 12 touchdown cycles (94°C, 30 sec; 60°C (0.5°C decrease for each cycle until 55°C), 30 sec; 72°C, 2 min), 35 regular cycles (94°C, 30 sec; 55°C, 30 sec; 72°C, 2 min) and a final incubation at 72°C for another 5 min. Aliquots (1 to 2 μ l) of unpurified PCR product were used for each sequencing reaction. The sequencing reaction was carried out from both directions using ABI Big Dye Terminator Sequencing Kits on an ABI 3700 capillary analyzer (Applied Biosystems).

SNP identification was completed using the ABI sequence software for base calling. Chromatograms were transferred to a sequence assembly software-Sequencher (Gene Codes, Ann Arbor, MI). Each base call was compared to the consensus sequence, and the variants were confirmed by visual inspection of the chromatograms.

Haplotype Analysis

Genotype results of the nine cSNPs from the panel of 44 individuals were used to estimate the haplotypes constructed out of these cSNPs. Haplotypes were determined using the “Haplotyper” algorithm (Niu et al., 2002). Specifically, the algorithm partitions the set of SNPs into smaller sets, estimating the phase for each of the smaller sets by a Gibbs sampler, then combining the adjacent sets using Gibbs sampler again to construct one level bigger haplotypes and thus continuing until the whole haplotype was estimated.

Construction of expression vectors for the reference and variant PEPT1s

The open reading frame of the human reference PEPT1 was first amplified from human small intestine QUICK-CLONE cDNA (Clontech) by *pfuTurbo* DNA polymerase (Stratagene, La Jolla, CA) and subcloned into Pcrii (Invitrogen, Carlsbad, CA). Then the cDNA fragment of human PEPT1 was constructed to contain BamH1 site at 5' side and Xba1 site at 3' side. Finally the fragment was introduced into BamH1/Xba1 sites of pcDNA3.1 expression vector (Invitrogen).

Point mutations were introduced into the constructed vector containing the reference PEPT1 using the QuickChange™ site-directed mutagenesis kit (Stratagene). Each variant PEPT1 in the vector was fully sequenced to ensure that only desired mutation was introduced.

Transfection, uptake study and Western analysis of the reference and variant PEPT1s

HeLa cells were seeded onto 24-well plates. When the cells reached 70-80% confluence, transfection was performed with FuGENE 6 (Roche, Indianapolis, IN) according to manufacturer's protocol. PEPT1-mediated [14 C]Gly-Sar uptake activity was measured in the cells cultured in 24-well plates 24-h post-transfection. The uptake medium was maintained at either pH 6.0 or pH 7.4 as described previously (Liang et al., 1995). Nonspecific uptake due to passive diffusion was determined in parallel experiments in HeLa cells transfected with the empty pcDNA3.1 vector. The cells were incubated for [14 C]Gly-Sar uptake for 3 min at room temperature. At the end of incubation, the cells were washed three times with ice-cold PBS (pH 7.4) and lysed in 0.3 ml/well of PBS with 1% Triton X-100 for 30 min. The aliquots were subjected to both liquid scintillation counting and protein quantification by the BCA protein assay kit. Uptake activity was determined as the number of pmols of Gly-Sar per mg of protein per 3 min.

In order to measure Gly-Sar transport kinetics, [14 C]Gly-Sar uptake in a concentration range of 0.094 to 3 mM was assessed with incubation time of 3 min, which is within the linear phase of the uptake process (the first 5 min). Passive diffusion (K_d , diffusion coefficient) was determined in parallel experiments in HeLa cells transfected with an empty pcDNA3.1 vector. Experimental data were fitted by KaleidaGraph (Synergy Software, Reading, PA), in which a model describing the uptake as a process combining diffusion and single site carrier-mediated transport (Liang et al., 1995) was used. The fitted kinetic parameters were presented as the maximal uptake velocity, V_{max} , and the

concentration, K_t , when uptake rate reaches half of V_{max} . All experiments were carried out in triplicate on two to three different experimental days.

For immunoblotting studies, the transfected HeLa cells were washed with PBS and lysed in lysing buffer as described (Wong et al., 1995). Lysates were diluted with Laemmli sample loading buffer, and separated by a 4-20 % SDS-polyacrylamide gel. Following transfer onto Immun-Blot PVDF membrane (Bio-Rad, Hercules, CA), blots were probed with anti-human PEPT1 (1:2000) or anti-calnexin (1:2000) antibodies, and visualized using a biotinylated anti-rabbit IgG and a chromogenic detection system (Vector Lab, Burlingame, VA).

Immunocytochemical analysis

HeLa cells were grown on the 4-well LAB-TEK Chambered Coverglass (Nalge Nunc International, Rochester, NY) and transfected with expression vectors containing the reference or P586L variant as described above. Cells were fixed in 1% formaldehyde in PBS for 10 min, permeabilized in PBS containing 0.025% NP-40 (Sigma-Aldrich) and 1% BSA for 15 min, and blocked with Protein Block (DAKO, Carpinteria, CA) for 30 min. Cells were then incubated with the rabbit anti-human PEPT1 antibody for 1 h at room temperature, washed three times with PBS containing 1% BSA, and incubated with Alexa Fluor488 goat anti-rabbit IgG (Molecular Probes, Eugene, OR) at a dilution of 1:500 in the antibody diluent (DAKO) for 1 h. Finally, cells were counterstained by 0.075 mM propidium iodide (Molecular Probes) in PBS for 5 min before visualization and analysis by Bio-Rad MRC1024-UV Confocal System (Bio-Rad, Hemel Hemstead, UK).

Quantitative real-time PCR

The mRNA expression level of each PEPT1 variant in comparison to the reference in transiently transfected HeLa cells was measured using SYBR green-based quantitative real time PCR. Specifically, transfected HeLa cells were washed with PBS 24-h post transfection, trypsinized and collected by centrifugation. Total RNA was extracted from cells by RNeasy Mini kit (Qiagen, Valencia, CA) according to manufacturer's protocol. Purified total RNA (8 µg) was digested by BamH1 and Xba1 restriction enzymes (Invitrogen) to linearize the residue plasmids post RNA isolation, followed by DNase-I treatment (DNA-free, Ambion, Austin, TX) according to manufacturer's instructions. First-strand cDNA was synthesized from treated RNA (1.5 µg) primed with random hexamers (150 ng), using SuperScript II RNase H⁻ Reverse Transcriptase (Invitrogen). Parallel control reactions were performed in the absence of reverse transcriptase (no-RT-control).

The internal standard curve was generated by using the reference PEPT1 cDNA diluted serially in DEPC-treated water, i.e. solutions of 3.75, 0.75, 0.1875, 0.0375 and 0.0075 ng RNA-equivalent cDNA/µl. All samples were diluted in DEPC-treated water to 0.75 ng RNA-equivalent cDNA/µl. PEPT1-specific primers are sense: *TTCTTCTCACCTGTGGCGAAG* and antisense: *TTGGAAGGAGCCTGAGAATATGA*. 18S rRNA was used as an endogenous control (sense: *CGGCTACCACATCCAAGGAA* and anti-sense: *GCTGGAATTACCGCGGCT*). Real-time PCR was performed in 20 µl volume containing 1 X SYBR Green PCR Master Mix (Applied Biosystems), 0.2 unit

AmpErase Uracil N-glycosylase (UNG from Applied Biosystems), 800 nM of each PEPT1-specific primers or 500 nM of 18S rRNA-specific primers, and 3 ng RNA-equivalent of cDNA. Real-time PCR reactions were set up in a 384-well plate by a robotic liquid handling system (Tecan U.S., Durham, NC). The expression levels of PEPT1 and 18S rRNA of each sample and standards were measured in separate amplification reactions in 5 replicates using an ABI Prism 7900HT Sequence Detection System (Applied Biosystems) under following cycling parameters: 50°C, 2 min; 95°C, 10 min, 40 cycles of 95°C, 15 sec and 60°C, 1 min. Sample of no-template-control and no-RT-control were also included in the sample 384-well plate. Each amplification included an endpoint melting curve analysis (60°C, 15 sec; 2% temperature ramp to 95°C, 15 sec) to identify non-specific amplification products (dissociation curve analysis).

Relative starting quantity of PEPT1 gene and 18S rRNA in each experimental sample was calculated from the standard curve method (Heid et al., 1996). Post-amplification, initial quantity of each cDNA was obtained by plotting cycle threshold (C_t) vs. quantity against known quantities of the standards. A mean of five identical replicates was used to calculate a single quantity value. The standard error of the mean (SEM) of the replicate wells were calculated for each PEPT1 sample and 18S rRNA. The relative expression level of each PEPT1 sample was calculated by normalizing the mean quantity of PEPT1 to the mean quantity of the 18S rRNA value. An overall SEM (δ) was derived using the delta method as described (Bishop et al., 1975):

$$\delta = \sqrt{\frac{(SEM_x)^2}{(m_y)^2} + \frac{(m_x)^2 \times (SEM_y)^2}{(m_y)^4}},$$

where m_x is the mean of PEPT1 quantity; m_y is the mean of 18S rRNA quantity;
 SEM_x is the SEM of PEPT1; and SEM_y is the SEM of 18S rRNA.

Results

Coding-region single-nucleotide polymorphisms in PEPT1

Upon screening a DNA polymorphism discovery panel comprising 44 individuals with different ethnicity, four synonymous and nine non-synonymous cSNPs in human PEPT1 gene were identified (Table 1). Genotyping raw data of the 44 individuals is available online as a data supplement to this article. According to a putative PEPT1 membrane topology model (Fig 1), most mutations occur on the extracellular loops, and two of non-synonymous SNPs are in the putative transmembrane regions. Many of these amino acids are highly conserved among PEPT1 orthologs and human PEPT2 (Fig 2).

Haplotype analysis was conducted on the nine non-synonymous cSNPs identified in this study. The estimated haplotypes are summarized in Fig 3. Ten haplotypes were deduced. The dominant (>62 %) haplotype is the one corresponding to the reference PEPT1 gene. The other haplotypes with relatively high estimated incidence are S117N (22.7%) and G419A (6.8%). The rest of haplotypes include some variants with double or triple mutations, and all of them are estimated to occur at relatively low frequency ($\leq 3.4\%$).

mRNA expression of the reference and PEPT1 variants in transfected HeLa cells

To determine the level of mRNA for each variant in comparison to the reference gene when transiently expressed in HeLa cells, quantitative RT-PCR was performed utilizing PEPT1-specific primers and 18s rRNA as an endogenous control. The amplification efficiency of PEPT1 gene and 18S rRNA were higher

than 90%, assessed by the slope and the linear regression ($R^2 \geq 0.99$) of their standard curves. Each PEPT1-related C_t value from the no-RT control RNA sample was sufficiently higher (> 9) than values obtained from each sample, and thus was not considered interfering with RNA analysis (data not shown). 18S rRNA expression level was invariable among different samples (C_t average was 9.17 ± 0.22). As shown in Fig 4, the mRNA level of each variant ranged from 1.6 to 2.2 fold of the reference level.

Functional analyses of PEPT1 variants in transfected HeLa cells

Using site-directed mutagenesis, expression vectors containing each PEPT1 variant were constructed. When transiently expressed in HeLa cells, the reference PEPT1 transported Gly-Sar in a pH-dependent manner (Fig 5A). This pH-dependent uptake was seen with the other variants, all of which transported Gly-Sar at a higher rate at pH 6.0 than at pH 7.4. Under the conditions used in this experiment, uptake rate of R459C was similar to the reference value, while uptake rates of the other variants (except for P586L) ranged from 1.3 to 1.6 fold of the reference value. Most distinctively, P586L showed a greatly reduced uptake rate ($p < 0.01$, Fig 5A).

Both anti-PEPT1 and anti-calnexin antibodies were used in western blot studies. The anti-PEPT1 antibody detected PEPT1-specific bands (~ 75 to ~ 100 kDa) in the cell extract from PEPT1 reference and variants (Fig. 5B), but not from the mock-transfected cells. In addition, it is evident that the immunoreactive protein level of P586L was lower than those of the reference and the other

variants, compared with the loading baseline provided by calnexin (Fig. 5C), which has been shown to be consistently expressed in transfected HeLa cells (Alvarez et al., 2003). This reduction in protein level appears consistent with the considerably diminished uptake rate of P586L (Fig 5A).

As shown in Fig 6, the same anti-PEPT1 antibody was used to detect PEPT1 expression in immunocytochemical analysis. The amplified green fluorescent signal was observed mostly on the cell membrane of transfected HeLa cells (Fig 6B, 6C), while some non-specific cytoplasmic staining could be observed with mock-transfected cells (Fig 6A). Moreover, the level of plasma membrane expression of the reference PEPT1 (Fig 6B) appeared much higher than that of the P586L variant (Fig 6C). These data, again, are in good agreement with the lower immunoreactive protein level of P586L (Fig 5B) as well as its diminished uptake rate (Fig 5A).

For a more comprehensive functional characterization, the concentration-dependent kinetics of Gly-Sar uptake was assessed for each PEPT1 variant. Determined by nonlinear curve fitting, the kinetic parameters are summarized in Table 2. All variants possessed K_t and V_{max} values similar to the reference, except for P586L, which retained a comparable K_t value, but had an approximately 10 fold lower V_{max} value ($p < 0.01$) than the reference and other variants.

For a further characterization of substrate recognition of each variant, seven previously reported PEPT1 drug substrates (Rubio-Aliaga and Daniel, 2002) were used to test relative inhibitory effects on Gly-Sar uptake by each

variant (Table 3). Glycine (negative control, 10 mM) showed minimal inhibition on [¹⁴C]Gly-Sar uptake by PEPT1 reference and variants, while unlabeled Gly-Sar (positive control, 10 mM) achieved nearly complete inhibition. The inhibition on Gly-Sar uptake by the reference and variants was similar for most drug substrates as demonstrated as the percentage of inhibition. To be specific: for bestatin, ALA and enalapril, each compound inhibited Gly-Sar uptake by all variants and the reference to a relatively high extent; for cefadroxil, captopril and cephalexin, each showed medium inhibitory effect on all variants and the reference; L-DOPA was the weakest inhibitor for all variants and the reference. Therefore, based on these information, we conclude that the selected seven drug substrates for human PEPT1 (reference) are likely to be substrates of all the PEPT1 variants, and the recognition of these drug substrates appear to be conserved among PEPT1 reference and variants.

To examine the phenotype of PEPT1 haplotypes, we also constructed the expression plasmids corresponding to the estimated haplotypes containing double or triple mutations (Fig 3), i.e. S117N/T451N, S117N/G419A/R459C, S117N/V416L and S117N/V122M/G419A. These double- or triple- altered variants retained similar pH-dependent Gly-Sar uptake as the reference and those of the variants with the single amino acid changes (data not shown). These data suggest that variants associated with Ser¹¹⁷, Val¹²², Val⁴¹⁶, Gly⁴¹⁹ and Arg⁴⁵⁹ did not alter PEPT1 function.

Discussion

Recently, a set of 24 membrane transporter genes was selected by the Pharmacogenetics of Membrane Transporters project (PMT) to be examined for genetic polymorphisms (Leabman et al., 2003). As a result, preliminary sequence information on some genetic variations of PEPT1 became public (www.pharmgkb.org); however, no functional data is available, and little can be surmised regarding whether these PEPT1 polymorphisms could lead to interindividual variability in oral absorption of PEPT1 drug substrates. In the current study, we screened a DNA panel composing 44 ethnically diverse individuals and found nine non-synonymous and four synonymous coding-region SNPs in human PEPT1. Then we studied the functional relevance of the non-synonymous cSNPs by using a heterologous expression system.

Our sequencing data is compared with preliminary data on PEPT1 from PMT project (Table 4). Although both DNA panels studied in our study and PMT project were from Coriell Institute, our panel, which is smaller in sample size, is not a subset of the DNA samples in PMT project. The two most common non-synonymous cSNPs, S117N and G419A, were identified in both studies with similar allelic frequency. In addition, three other non-synonymous cSNPs (V122M, V450I and T451N) and all four synonymous cSNPs identified in our study were also found in the PMT project, although with different frequencies. However, all low frequency cSNPs ($\leq 0.4\%$, occurring in one or two chromosomes in the total of 247 subjects) in PMT dataset were not found in our study. The converse is true for three low-frequent cSNPs including T114I, R459C and

P586L ($\leq 1.1\%$), identified in our study, each of which occurred once in the total of 88 chromosomes. It appears that the smaller sample size of 44 individuals screened in our study is sufficient to identify major PEPT1 variants, since all of the relatively high-frequent cSNPs found in our study matched well with the results from the PMT project. However, surprisingly, three low-frequent non-synonymous cSNPs (T114I, R459C and P586L) were found in our subjects, but not in PMT project. Further, a re-sequencing effort on the individual DNA samples with these PEPT1 variations has ruled out the possibility of sequencing error.

When the transport function of the identified nine non-synonymous variants was assessed in vitro in comparison to the reference PEPT1 gene, all variants including P586L, similar to the reference, possessed the higher uptake rate at the lower pH value (Fig 5A). This retained pH-dependency on Gly-Sar uptake indicates that these codon changes appear not to occur in PEPT1 regions essential for proton co-transport. Kinetic studies revealed comparable K_t values for Gly-Sar uptake by all variants and the reference (Table 2). In order to further assess whether this conserved substrate recognition can be seen with drug substrates, seven chemically diverse compounds, including β -lactams antibiotics (cefadroxil and cephalexin), angiotensin-converting enzyme (ACE) inhibitors (captopril and enalapril), peptidomimetic drugs (bestatin), and non-peptidic substrates (L-DOPA and 5-aminolevulinic acid), were selected. A single concentration (10 mM) for all drug substrates was chosen in the uptake inhibition study. At this tested concentration, the inhibitory effect of each compound could

be roughly categorized as relatively high, medium and low (see “*results*”). Table 3 demonstrated that the inhibition ranking of each drug substrate observed in the reference PEPT1 was, by and large, similarly seen among all the variants. Therefore, collectively, these results suggest that all variants likely retain a substrate-recognition/binding pocket similar to the reference PEPT1.

One interesting finding in the study was the reduced uptake capacity of variant P586L. This variant retains pH-dependent uptake, but with significantly reduced capacity. Kinetic studies revealed that P586L has similar K_t to Gly-Sar as the reference and other variants, but with a transport capacity ten-fold less as measured by V_{max} . In addition, the inhibitory effect by the selected drug substrates on Gly-Sar uptake by P586L was similar to that observed with the other variants. Western blot analysis on whole cell lysate (Fig 5B) demonstrated that P586L was expressed at a much lower level in comparison to the reference in transfected HeLa cells. Further immunocytochemical studies confirmed that membrane expression level of P586L was indeed lower than that of the reference. Therefore, the lower transport capacity (V_{max}) observed in P586L is likely the result of the lower transporter density on cell membrane, and not due to intrinsic changes in transport function. Since protein expression is controlled by both transcriptional and translational/post-translational mechanisms, we performed a real time PCR study to assess if there was any alteration on mRNA expression level of each variant, which may account for the changes on protein expression level (especially for P586L). Results (Fig 4) suggested that all variants (including P586L) showed slightly higher mRNA level than the reference

gene in the transient transfected cell system. Therefore, the significant reduction of P586L protein expression level appears not to be attributed to variations on gene transcription, but mainly due to alterations occurring post-transcriptionally. Given that Pro⁵⁸⁶ is located on the putative membrane boundary of the transmembrane (TM) domain and could be an essential residue for α -helix packing of TM domain (Brandl and Deber, 1986), we propose that substitution of proline with leucine at position 586 may have profound effect on protein stability or translational control, which leads to low protein expression level on the cell membrane. Experiments to determine the effect of P586L on post-transcriptional events are beyond the scope of this study and are the subject of future work.

When utilizing site-directed mutagenesis to study protein structure-function relationships, it is assumed that important amino acids are conserved in the protein family and changes in conserved residues should affect protein function. Similarly, this reasoning should stand, when it comes to determining whether a non-synonymous SNP of a given transporter can alter transport function and lead to a functional consequence. As shown in Fig 3, we created sequence alignments for partial regions in hPEPT1 containing the nine cSNPs and sequences from 6 animal species and human PEPT2. Some of the SNPs resulted in replacement of a conserved amino acid by a different amino acid present in another species in the same position (i.e. S117N and T451N). Gly⁴¹⁹ was not conserved cross species, while the substituted alanine is observed in rat and mouse PEPT1. Based on this alignment, we expected that these three cSNPs (S117N, T451N and G419A) should be functionally neutral; while the

other cSNPs occurring at conserved positions would have a greater probability of resulting in a functional consequence, depending on the type of substituting residue. For example, P586L may have altered function, since Pro⁵⁸⁶ is in an evolutionarily conserved region, and the substituting Leu is structurally different from Pro. Recently, a computational method was proposed to predict the cSNPs that might have a functional consequence. This program, SIFT (Sorting Intolerant from Tolerant)(Ng and Henikoff, 2002), is actually a sequence homology based tool that evaluates whether amino acid changes are conserved within the protein family to predict which cSNPs would affect protein function. SIFT predicted that most PEPT1 cSNPs identified were tolerated mutations, except for P586L (Data not shown). Not surprisingly, our experimental results on P586L concurred with the prediction from this sequence homology based analysis.

Despite the efforts to elucidate the structure-function relationship of PEPT1, the exact PEPT1 protein domains important for proton-coupling and substrate-translocation remain elusive in the absence of a high-resolution three-dimensional X-ray structure (Zhang et al., 2002). To date, some amino acid residues or domains in PEPT1 have been revealed functionally important, and the results in the present study are largely compatible with those earlier findings: (1) Previous studies on PEPT1 and PEPT2 chimeras (Doring et al., 1996) suggested that the large extracellular loop between TM9 and TM10 is not essential for phenotypical characteristics of transporter function. This observation is in good agreement with our results: five cSNPs located on this loop have little influence on transporter function in terms of pH-dependency, substrate uptake

kinetics and inhibition specificity. (2) Previous site-directed mutagenesis studies on human PEPT1 have revealed five functionally important conserved residues, which are all located in putative transmembrane (TM) domains. Specifically, two histidine residues, i.e. His⁵⁷ and His¹²¹ (Chen et al., 2000), are on TM2 and TM4, respectively; Tyr¹⁶⁷ is on TM5 (Bolger et al., 1998; Yeung et al., 1998); Try²⁹⁴ is on TM7 and Glu⁵⁹⁵ is on TM10 (Bolger et al., 1998). When human PEPT1 was mutated at each of these sites, transport function was lost or significantly diminished. In addition to identification of those functionally important residues in PEPT1, it has been proposed that the N-terminal half including TM7, TM8 and TM9 is the region of PEPT1 responsible for proton and substrate recognition (Doring et al., 1996; Fei et al., 1998; Terada et al., 2000), and a recent study with cysteine-mutagenesis on PEPT1 revealed that TM5 may be part of the substrate translocation pathway (Kulkarni et al., 2003). Additionally, it has been speculated that the C-terminal region, although not directly involved in substrate recognition and binding, may be important for either protein trafficking or functional regulation (Doring et al., 1996). Located on the membrane boundary of TM10 in C-terminal portion of PEPT1, Pro⁵⁸⁶ was shown not to be important for protein function in terms of pH-dependent uptake, Gly-Sar affinity and inhibitor specificity, as P586L behaved similarly to the reference gene with respect to these parameters. However, Pro⁵⁸⁶ appeared important in determining PEPT1 expression level in the membrane. Coincidentally, the Ala substituted mutant on another conserved residue in the TM10, Glu⁵⁹⁵, retained the K_t value similar to the wild-type PEPT1, but had significantly reduced transport capacity (V_{max}) in transfected HEK cells

(Bolger et al., 1998). Although no experiment was carried out to assess the expression level of E595A, we speculate, in the context of the present study, that the low transport capacity (V_{max}) of E595A may be associated with lower incorporation of the protein in the membrane. Taken together, these results provide supporting evidence for the concept (Doring et al., 1996) regarding the potential role of C-terminal to PEPT1 function, i.e. regulating transporter expression level. Further analyses are required to determine how these residues in the C-terminal region of PEPT1 modulate the expression level of PEPT1.

Although P586L appears to be associated with a decrease in V_{max} in transfected HeLa cells, we speculate that the reduction of uptake capacity *in vitro* may not be consequential *in vivo*, given that PEPT1 is expressed at a high level along the gastrointestinal tract (Ganapathy and Leibach, 1996). The fact that no mutation identified in the studied subjects that resulted in complete loss of hPEPT1 function may reflect the strong selection and evolutionary pressure on this important mammalian peptide transporter, which has counterparts in bacteria, yeast, fungi, plants, invertebrate and vertebrate animals. Therefore the maintenance of appropriate di/tri-peptide cellular uptake appears essential for the well-being of all living creatures.

In this study, we reported the identification and *in vitro* functional characterization of human PEPT1 variants. Analyses of these cSNPs revealed that the mutations appear to be functionally neutral except for P586L, which maintained a similar affinity for Gly-Sar and drug substrates as the other variants but had reduced protein expression in transfected HeLa cells. These data

suggest that the C-terminal region of PEPT1 (where Pro⁵⁸⁶ resides) appears to be involved in regulation on PEPT1 expression, which is consistent with previous studies. However, the P586L allele appears to be a rare variant (found in one chromosomes out of 44 subjects in our study; but not found in another larger group of subjects, i.e. 247 individuals in PMT study) and therefore would have minimal impact on oral absorption of PEPT1 drug substrates. In conclusion, human PEPT1 transport functionality appears to be highly conserved, and PEPT1 polymorphisms are not expected to be a significant factor with respect to intersubject variability in oral absorption of its drug substrates.

Acknowledgements

We thank Anne Dantzig for critical reading of the manuscript, Sandra Kirkwood and Michael Flagella for discussion, Mike Esterman and Xiaoling Xia for technical support.

Reference

- Alvarez C, Garcia-Mata R, Brandon E and Sztul E (2003) COPI recruitment is modulated by a Rab1b-dependent mechanism. *Mol Biol Cell* **14**:2116-2127.
- Balimane PV, Tamai I, Guo A, Nakanishi T, Kitada H, Leibach FH, Tsuji A and Sinko PJ (1998) Direct evidence for peptide Transporter (PepT1)-mediated uptake of a nonpeptide prodrug, valacyclovir. *Biochem and Biophys Res Commun* **250**:246-251.
- Bishop Y, Feinberg S and Holland P (1975) *Discrete Multivariate Analysis: Theory and Practice*. The MIT Press, Cambridge.
- Bolger MB, Haworth IS, Yeung AK and H. LV (1998) Structure, function, and molecular modeling approaches to the study of the intestinal dipeptide transporter PepT1. *J Pharm Sci* **87**:1286-1291.
- Brandl CJ and Deber CM (1986) Hypothesis about the function of membrane-buried proline residues in transport proteins. *Proc Natl Acad Sci USA* **83**:917-921.
- Chen X-Z, Steel A and Hediger MA (2000) Functional roles of histidine and tyrosine residues in the H⁺-peptide transporter PepT1. *Biochem and Biophys Res Commun* **272**:726-730.
- Dantzig AH (1997) Oral absorption of [beta]-lactams by intestinal peptide transport proteins. *Adv Drug Delivery Rev* **23**:63-76.
- Doring F, Dorn D, Bachfischer U, Amasheh S, Herget M and Daniel H (1996) Functional analysis of a chimeric mammalian peptide transporter derived from the intestinal and renal isoforms. *J Physiol* **497**:773-779.

Fei YJ, Kanai Y, Nussberger S, Ganapathy V and Hediger MA (1994) Expression cloning of a mammalian proton-coupled oligopeptide transporter. *Nature* **368**:563-566.

Fei Y-J, Liu J-C, Fujita T, Liang R, Ganapathy V and Leibach FH (1998) Identification of a potential substrate binding domain in the mammalian peptide transporters PEPT1 and PEPT2 Using PEPT1-PEPT2 and PEPT2-PEPT1 chimeras. *Biochem and Biophys Res Commun* **246**:39-44.

Fei Y-J, Sugawara M, Liu J-C, Li HW, Ganapathy V, Ganapathy ME and Leibach FH (2000) cDNA structure, genomic organization, and promoter analysis of the mouse intestinal peptide transporter PEPT1. *Biochim Biophys Acta - Gene Structure and Expression* **1492**:145-154.

Friedrichsen GM, Nielsen CU, Steffansen B and Begtrup M (2001) Model prodrugs designed for the intestinal peptide transporter. A synthetic approach for coupling of hydroxy-containing compounds to dipeptides. *Eur J Pharm Sci* **14**:13-19.

Ganapathy V and Leibach F (1996) Peptide transporters. *Curr Opin Nephrol Hypertens* **5**:395-400.

Hayes J and Strange R (2000) Glutathione S-transferase polymorphisms and their biological consequences. *Pharmacology* **61**:154-166.

Heid C, Stevens J, Livak K and Williams P (1996) Real time quantitative PCR. *Genome Res* **6**:986-994.

- Ho ES, Lin DC, Mendel DB and Cihlar T (2000) Cytotoxicity of antiviral nucleotides adefovir and cidofovir is induced by the expression of human renal organic anion transporter 1. *J Am Soc Nephrol* **11**:383-393.
- Hoffmeyer S, Burk O, von Richter O, Arnold HP, Brockmoller J, John A, Cascorbi I, Gerloff T, Roots I, Eichelbaum M and Brinkmann U (2000) Functional polymorphisms of the human multidrug-resistance gene: Multiple sequence variations and correlation of one allele with P-glycoprotein expression and activity in vivo. *Proc Natl Acad Sci USA* **97**:3473-3478.
- Ito S, Ieiri I, Tanabe M, Suzuki A, Higuchi S and Otsubo K (2001) Polymorphism of the ABC transporter genes, MDR1, MRP1 and MRP2/cMOAT, in healthy Japanese subjects. *Pharmacogenetics* **11**:175-184.
- Kim RB, Leake BF, Choo EF, Dresser GK, Kubba SV, Schwarz UI, Taylor A, Xie H-G, McKinsey J and Zhou S (2001) Identification of functionally variant MDR1 alleles among European Americans and African Americans. *Clin Pharmacol Ther* **70**:189-199.
- Kulkarni AA, Haworth IS and Lee VHL (2003) Transmembrane segment 5 of the dipeptide transporter hPepT1 forms a part of the substrate translocation pathway. *Biochem and Biophys Res Commun* **306**:177-185.
- Leabman M, Huang C, Kawamoto M, Johns S, Stryke D, TE F, J D, Taylor T, Clark A, Herskowitz I and Giacomini K (2002) Polymorphisms in a human kidney xenobiotic transporter, OCT2, exhibit altered function. *Pharmacogenetics* **12**:395-405.

Leabman MK, Huang CC, DeYoung J, Carlson EJ, Taylor TR, de la Cruz M, Johns SJ, Stryke D, Kawamoto M, Urban TJ, Kroetz DL, Ferrin TE, Clark AG, Risch N, Herskowitz I, Giacomini KM and Pharmacogenetics of Membrane Transporters Investigators (2003) Natural variation in human membrane transporter genes reveals evolutionary and functional constraints. *Proc Nat Acad Sci USA* **100**:5896-5901.

Liang R, Fei Y-J, Prasad PD, Ramamoorthy S, Han H, Yang-Feng TL, Hediger MA, Ganapathy V and Leibach FH (1995) Human intestinal H⁺/peptide cotransporter. *J Biol Chem* **270**:6456-6463.

Mackenzie P, Miners J and McKinnon R (2000) Polymorphisms in UDP glucuronosyltransferase genes: functional consequences and clinical relevance. *Clin Chem Lab Med* **38**:889-892.

Meyer U and Zanger U (1997) Molecular mechanisms of genetic polymorphisms of drug metabolism. *Annu Rev Pharmacol Toxicol* **37**:269-296.

Ng PC and Henikoff S (2002) Accounting for human polymorphisms predicted to affect protein function. *Genome Res* **12**:436-446.

Nishizato Y, Ieiri I, Suzuki H, Kimura M, Kawabata K, Hirota T, Takane H, Irie S, Kusuvara H and Urasaki Y (2003) Polymorphisms of OATP-C (SLC21A6) and OAT3 (SLC22A8) genes: Consequences for pravastatin pharmacokinetics. *Clin Pharmacol Ther* **73**:554-565.

Niu T, Qin Z, Xu X and Liu JS (2002) Bayesian Haplotype Inference for Multiple Linked Single-Nucleotide Polymorphisms. *Am J Hum Genet* **70**:157-169.

Rodrigues A and Rushmore T (2002) Cytochrome P450 pharmacogenetics in drug development: in vitro studies and clinical consequences. *Curr Drug Metab* **3**:289-309.

Rubio-Aliaga I and Daniel H (2002) Mammalian peptide transporters as targets for drug delivery. *Trends Pharmacol Sci* **23**:434-440.

Sababi M, Borga O and Hultkvist-Bengtsson U (2001) The role of P-glycoprotein in limiting intestinal regional absorption of digoxin in rats. *Eur J Pharm Sci* **14**:21-27.

Saito H, Okuda M, Terada T, Sasaki S and Inui K (1995) Cloning and characterization of a rat H⁺/peptide cotransporter mediating absorption of beta-lactam antibiotics in the intestine and kidney. *J Pharmacol Exp Ther* **275**:1631-1637.

Steffansen B, Lepist E-I, Taub ME, Larsen BD, Frokjaer S and Lennernas H (1999) Stability, metabolism and transport of -Asp(OBzl)-Ala -- a model prodrug with affinity for the oligopeptide transporter. *Eur J Pharm Sci* **8**:67-73.

Terada T, Saito H, Sawada K, Hashimoto Y and Inui K (2000) N-terminal halves of rat H⁺/peptide transporters are responsible for their substrate recognition. *Pharm Res* **17**:15-20.

Thomsen AE, Friedrichsen GM, Sorensen AH, Andersen R, Nielsen CU, Brodin B, Begtrup M, Frokjaer S and Steffansen B (2003) Prodrugs of purine and pyrimidine analogues for the intestinal di/tri-peptide transporter PepT1: affinity for hPepT1 in Caco-2 cells, drug release in aqueous media and in vitro metabolism. *J Controlled Release* **86**:279-292.

- Tirona RG, Leake BF, Merino G and Kim RB (2001) Polymorphisms in OATP-C. Identification of multiple allelic variants associated with altered transporter activity among European- and African-Americans. *J Biol Chem* **276**:35669-35675.
- Tokui T, Nakai D, Nakagomi R, Yawo H, Abe T and Sugiyama Y (1999) Pravastatin, an HMG-CoA reductase inhibitor, is transported by rat organic anion transporting polypeptide, oatp2. *Pharm Res* **16**:904-908.
- Wong MH, Oelkers P and Dawson PA (1995) Identification of a mutation in the ileal sodium-dependent bile acid transporter gene that abolishes transport activity. *J Biol Chem* **270**:27228-27234.
- Yeung AK, Basu SK, Wu SK, Chu C, Okamoto CT, Hamm-Alvarez SF, Grafenstein Hv, Shen W-C, Kim K-J and Bolger MB (1998) Molecular identification of a role for tyrosine 167 in the function of the human intestinal proton- coupled dipeptide transporter (hPepT1). *Biochem Biophys Res Commun* **250**:103-107.
- Zhang EY, Phelps MA, Cheng C, Ekins S and Swaan PW (2002) Modeling of active transport systems. *Adv Drug Delivery Rev* **54**:329-354.

Table 1. Summary of cSNPs in the human PEPT1 gene. *, SNP identification numbers are designated according to the corresponding Exon No. The non-synonymous cSNPs are *underlined*.

Table 2. Kinetic parameters for [¹⁴C]Gly-Sar uptake by PEPT1 variants.

Uptake of [¹⁴C]Gly-Sar by transfected HeLa cells at pH 6.0 was determined over a concentration range of 0.094-3 mM. Parameters were calculated from two to three independent studies completed in triplicates and obtained as described under “*Methods*”. K_d fitted from the uptake rate-concentration profile by HeLa cells transfected with empty pcDNA3.1 vector was 0.56 ± 0.03 . K_t and V_{max} were shown in mean \pm S.E. * $p < 0.01$.

Table 3. Gly-Sar uptake Inhibition in PEPT1 transfected HeLa cells. The uptake of [¹⁴C]Gly-Sar (50 μ M) was measured at pH 6.0 with the incubation time of 3 min. Concentration of each inhibitor was 10 mM. Uptake values were subtracted by the background value (uptake by cells transfected with empty vector) and were presented as % of inhibition. Each value was calculated from four to six measurements, and shown as the mean value (S.E. varies from 2% to 7% of the mean).

Table 4. Comparisons of cSNPs identified in this study and the PMT project. The allelic frequency was calculated as the percentage with 44 subjects

used in the present study and 247 subjects from the PMT project. Non-synonymous SNPs were *underlined*. *: SNP identified only in this study; **: SNP identified only in the PMT project. ND: not detected.

Legends for figures

Fig 1. Schematic representation of PEPT1 cSNPs. Non-synonymous amino acid changes are *numbered* and shown in *dark* circles; synonymous changes in *gray* circles.

Fig 2. Partial primary sequence alignments of PEPT1 from various species and human PEPT2. Non-synonymous SNPs were indicated. Created by AlignX module in Vector NTI 7.0 (Informax, Frederick, MD).

Fig 3. Schematic of PEPT1 allelic variant identified in the study.

Haplotype analysis was performed by using Haplotyper as described in *Methods*. Non-synonymous mutations are shown in *boxes*.

Fig 4. Assessment of each PEPT1 variant mRNA level relative to the reference level in transfected HeLa cells by Real time PCR. Followed transient transfection, HeLa cells were collected, and total RNA were extracted. The mRNA level of HeLa cells transfected by empty vector (Control) and vectors containing PEPT1 variants was quantified using PEPT1-specific primers and 18S rRNA as endogenous control. The mRNA level of the reference was set as 100. The mean of each 5 replicate level is plotted and the error bars represent overall SEM (δ), calculated as in *Methods*.

Fig 5. Expression of the reference and PEPT1 variants in HeLa cells. (A) pH-dependent Gly-Sar uptake. Transfection was conducted by using FuGENE 6. PEPT1-mediated [^{14}C]Gly-Sar (50 μM) uptake activity was measured in the cells in 24-well plates under two pH conditions (6.0 and 7.4). Cells transfected with the

empty pcDNA3.1 vector was served as *control*. Data are shown as mean \pm S.E. (B), (C) Immuno-blot analyses. Electrophoreses were run in parallel. The blots were probed with a rabbit anti-human PEPT1 (B) or anti-calnexin (C) polyclonal antibodies and visualized using a biotinylated anti-rabbit IgG and a chromogenic detection system.

Fig 6. Immunocytochemical detection of PEPT1 in transfected HeLa cells.

HeLa cells were transfected with (A) empty vector, (B) reference sequence, and (C) P586L. Expressed proteins were visualized by Alexa Fluor 488 shown in *green*. Nuclei were stained by propidium iodide shown in *red*. Green fluorescent molecules, Alexa 488, were excited with a Krypton/Argon laser at 488 ± 10 nm, and the emission was detected at 522 ± 17 nm; Red fluorescent molecules, Propidium iodide, were excited with a 568 nm Krypton/Argon line, and the emission was detected at ≥ 585 nm.

Table 1.

SNP ID.*	Nucleotide sequence	Effect
5.1	5' TGGCA [C/T] CCCC 3'	<u>T114I</u>
5.2	CGACA [G/A] CCTTC	<u>S117N</u>
5.3	TGCAC [G/A] TGTGA	<u>V122M</u>
16.2	GGAAA [C/T] GAAGT	N393
16.3	AGATG [G/C] TGACA	<u>V416L</u>
16.4	ACTTG [G/C] CCCAA	<u>G419A</u>
17.1	ACTGC [C/T] GTAAC	A449
17.2	CTGCC [G/A] TAACT	<u>V450I</u>
17.3	CGTAA [C/A] TGACG	<u>T451N</u>
17.4	GCCAA [C/T] GCCAC	<u>R459C</u>
18.2	CCAGA [A/G] AAAGG	E482
19.1	GCAAA [C/T] ATCAG	N509
21.4	AATCC [C/T] GCAGT	<u>P586L</u>

Table 2

Variants	K_t (mM)	V_{max} (nmol/mg/3 min)
Reference	0.33 ± 0.10	14.9 ± 2.2
T114I	0.32 ± 0.08	12.0 ± 2.7
S117N	0.43 ± 0.10	14.8 ± 2.0
V122M	0.65 ± 0.17	19.5 ± 2.6
V416L	0.38 ± 0.05	16.1 ± 1.8
G419A	0.45 ± 0.08	18.5 ± 2.6
V450I	0.35 ± 0.06	12.9 ± 1.6
T451N	0.35 ± 0.05	14.1 ± 0.6
R459C	0.32 ± 0.07	16.4 ± 1.1
P586L	0.25 ± 0.09	$1.34 \pm 0.3^*$

Table 3

Inhibitor	% of Inhibition									
	Ref	T114I	S117N	V122M	V416L	G419A	V450I	T451N	R459C	P586L
Glycine	4	1	1	0	1	0	2	0	0	5
Gly-Sar	96	93	95	94	95	94	93	94	95	96
Bestatin	99	96	95	97	96	94	96	94	96	96
ALA	89	90	87	88	87	87	85	84	86	76
Enalapril	87	93	89	95	92	91	94	90	92	90
Cefadroxil	73	76	62	70	65	70	72	69	66	61
Captopril	61	64	52	64	53	52	57	49	50	41
Cephalexin	53	38	48	40	39	31	35	34	29	31
L-DOPA	37	21	28	21	13	15	14	13	22	12

Table 4

SNP	Allelic frequency	
	Present	PMT project
<u>S117N</u>	0.295	0.250
<u>V122M</u>	0.011	0.008
N393	0.023	0.012
<u>G419A</u>	0.091	0.081
A449	0.295	0.137
<u>V450I</u>	0.011	0.014
<u>T451N</u>	0.034	0.012
E482	0.034	0.006
N509	0.080	0.094
<u>T114I</u> *	0.011	ND
<u>V416L</u> *	0.011	ND
<u>P586L</u> *	0.011	ND
<u>V21I</u> **	ND	0.002
<u>F28Y</u> **	ND	0.002
S86 **	ND	0.002
N110 **	ND	0.004
<u>S117R</u> **	ND	0.002
T281 **	ND	0.002
<u>P537S</u> **	ND	0.002
S616 **	ND	0.002

Fig 1

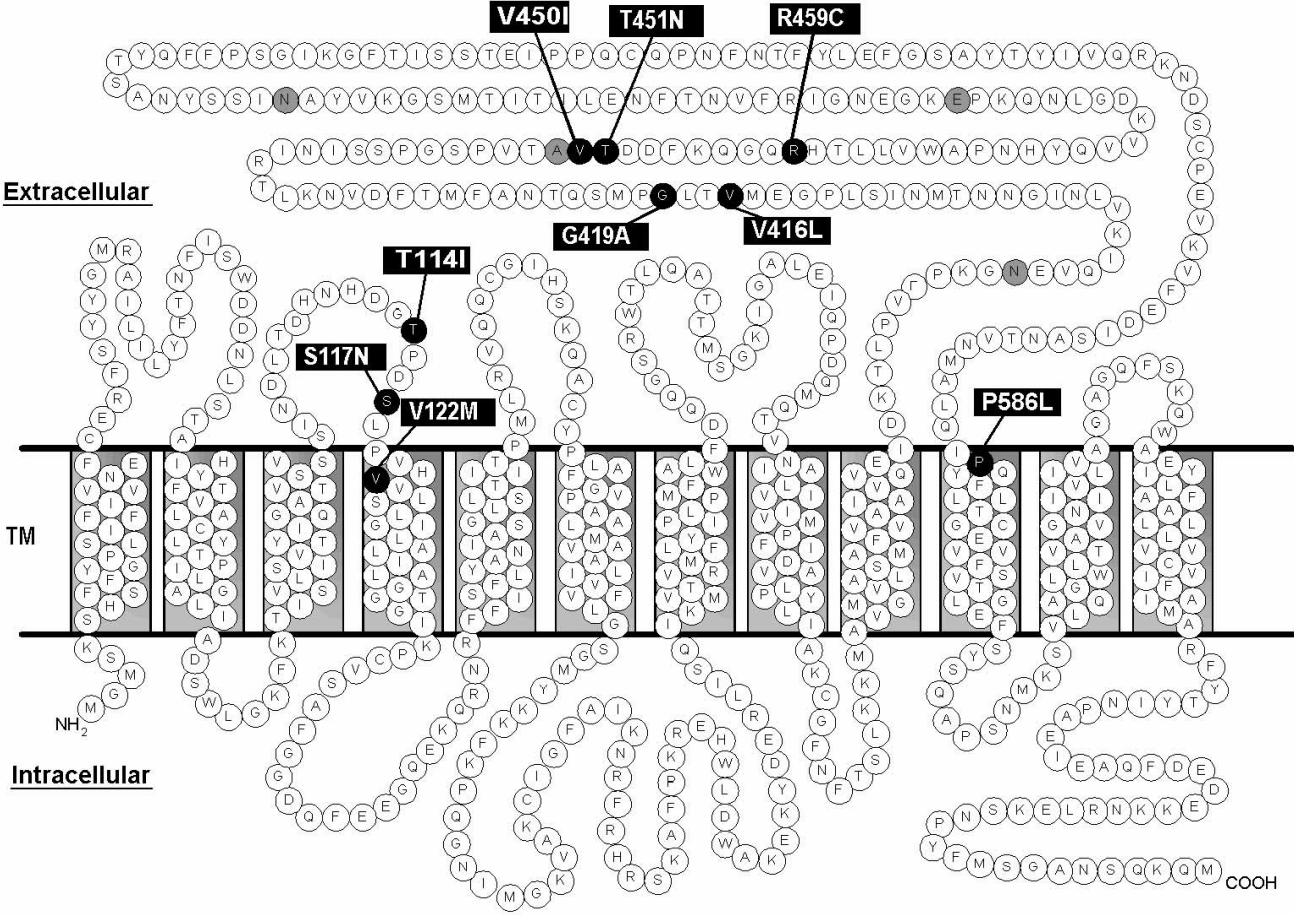


Fig 2

	-T114I	-S117N	-V122M	-V416L	-G419A	-V450I	-I451N	-R459C	-P586L
Human	DGTPDSL	LPVHVVL		EMVTLGPM		AVTDDFKQGQRHT			QIPQY
Monkey	DGTPDSL	LPVHVAL		EMVTLDSL		AVTDDFKQGQRHT			QIPQY
Rabbit	DGTPDSL	LPVHVAV		QTVTLNQM		MITPSLEAGQRHT			QIPQY
Dog	DGTPDNL	SVHVAL		AVVTVSQM		PVTYNFEQGHRHT			QIPQY
Rat	DGSPNNL	LHVAL		KNVTVAQM		TVAHEFEPGHRHT			QIPQY
Mouse	NGSPDSL	LPVHVAL		NSVTLAQM		TVAHDFEQGHRHN			QIPQY
Chicken	DGNPDN	LAVHIAL		QNVTVLPM		SENIDSSISNTHT			QIPQY
HuPEPT2	-----	GQVVHTVL		LIESIKSF		LYTEHSVQEKWY			QLPQY

Fig 3

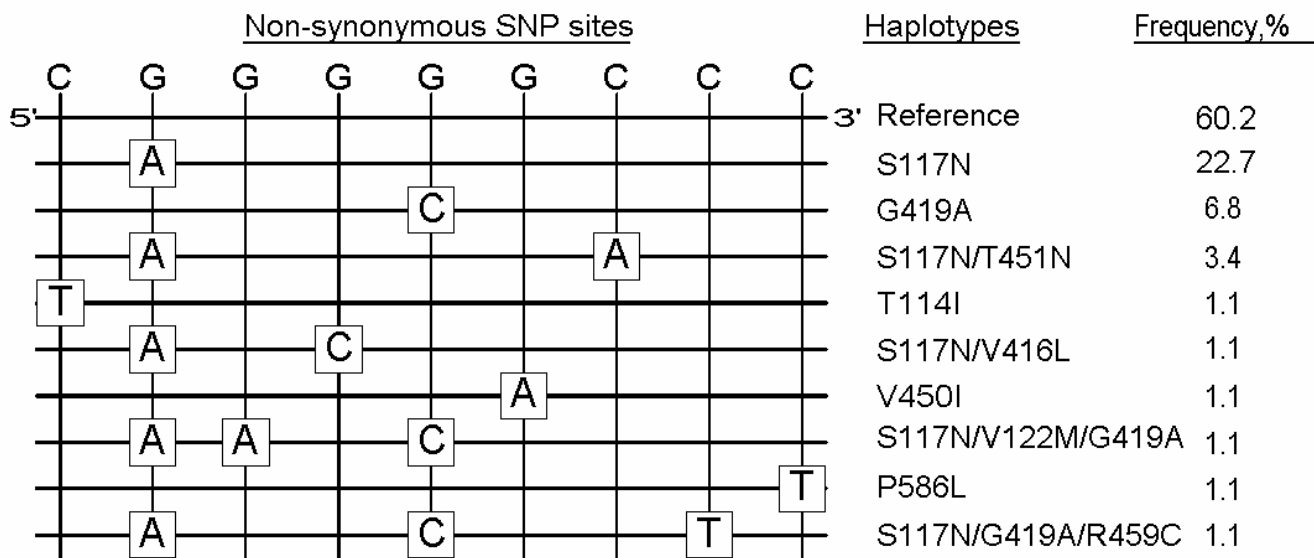


Fig 4

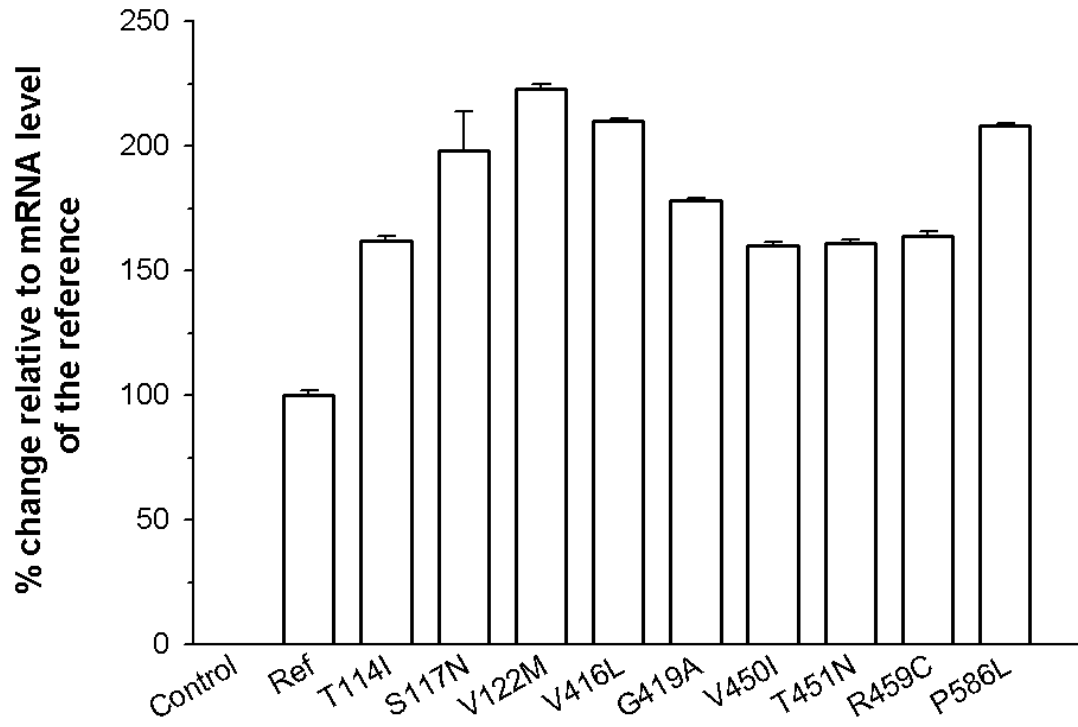
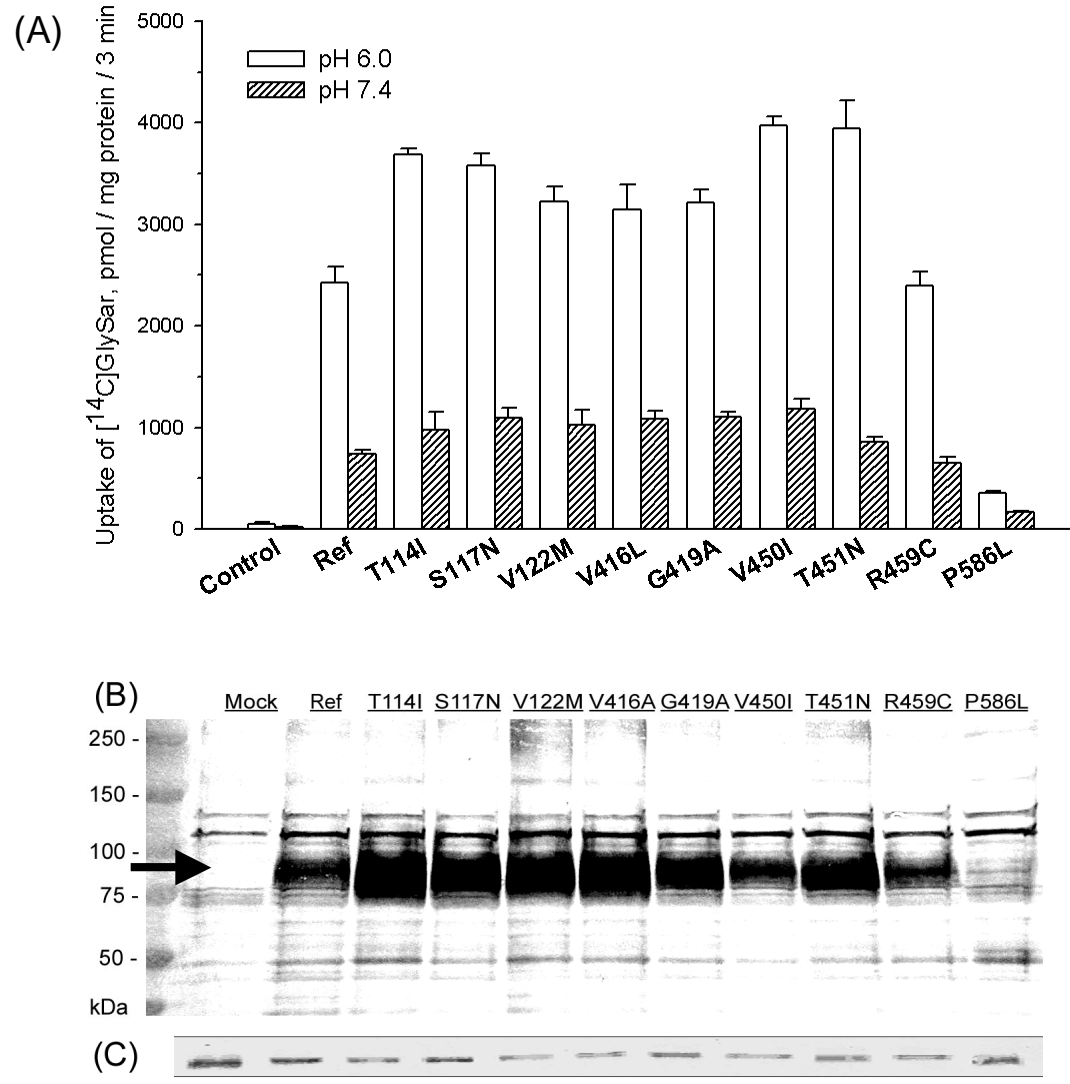


Fig 5



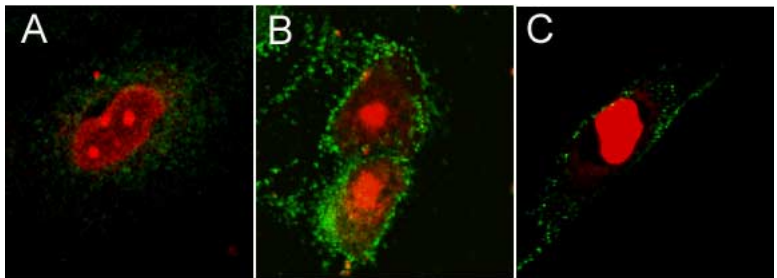


Fig 6